Australian Journal of Basic and Applied Sciences, 5(10): 513-519, 2011
ISSN 1991-8178

Analysis of the Optimal Condition of Differential Digital Speckle Pattern Inteferometry

Nasser A.Moustafa

Department of Physics, Faculty of Science, Helwan University, Ain Helwan, Cairo, Egypt.

Abstract: A theoretical investigation of the optimal signal processing in DDSPI using the double reference beam technique is presented. Optical noise is taken care of, and the optimum of DDSPI with regard to reference/object-ratio is found. The dependence of the optimal reference to object intensity ratio on spurious noise patterns in the reference beam is given.

Key words: Speckle pattern, speckle interferometry, difference correlation fringes, comparative measurement, fringe signal.

INTRODUCTION

Interferometry can be used to produce a fringe pattern that represents the field surface displacement of an object in response to some change in mechanical loading (Nakadate, 1980). Digital speckle pattern interferometry (DSPI) is one of the most modern techniques for depicting such fringe patterns. It combines real-time processing with the flexibility of software handling. DSPI was developed by combining the well-known techniques of holographic and speckle interferometry by using an image hologram setup and following the methods of double-exposure holography. It utilizes a CCD camera interfaced to a computer to process the data. For comparison measurements, a reference frame stored in memory is continuously subtracted from incoming data, and then the intensity difference is displayed. The fringes represent the correlation between the speckle patterns (Creath, 1985; János Kornis, 1997; Ganesan, 1987) In our investigation, the light scattered from the master object is used as reference beam.

The comparison process can be made between the light scattered from the master and test object. Little has been published about the optimal condition of ESPI. Pederson *et al*. explain qualitatively how the signal is treated and when the optimal condition is reached. They also point out the importance of the optical noise to the reference beam. EK *et al*. (1979) discuss the fringe contrast with low resolution imaging devices. EK and Biedermann (László, 1997) presented a related analysis of fringe contrast in hologram interferometry in which a double slit aperture was used to improve the fringe contrast. G.A.Sletemoen (Lászlo, 1996) determine the optimal reference to object intensity ratio, which maximizes the fringe signal, and the dependence on the size of the aperture is given. The effect of a double slit aperture is compared with the effect of a circular aperture. In this paper we aim to investigate the optimal signal processing in the digital speckle pattern interferometry (DSPI). The optimal reference-to-object intensity ratio is determined and the dependence on the spurious noise in the reference field which point out that it cause a trouble.

2. The Analysis of the Interference Patterns:

The schematic diagram of the experimental setup is shown in Fig.1. A and B are two objects, the master one consisted of two areas, one is movable and the other is fixed (Fig.2). The test object consists of one area, which is movable (Fig. 3). The movement of the master and the test objects is axially.

The first experiment performed by using only the movable area. In the first step we recorded the undeformed state of the illuminated test object and the undeformed state of the illuminated master object. In the second step we recorded the deformed state of the illuminated test object and the deformed state of the illuminated master object, and stored them in the memory of the computer. The result of subtraction is the difference correlation fringes. The second experiment performed by using the technique as before with the only difference that we made a modification by adding a fixed area for the movable area of the master object. In the first step we recorded the wave fields scattered by the test object in its undeformed state and the wave field scattered by the modified master in its undeformed state. The simple treatment of the process is as follow:

U_m, and U_r are the complex amplitudes of the wave fields scattered by the movable (undeformed), and fixed areas of the modified master object respectively.

U_{mr} is the resultant complex amplitude of the wave fields scattered by the movable (undeformed), and fixed areas of the modified master object.

Corresponding Author: Nasser A.Moustafa, Department of Physics, Faculty of Science ,Helwan University, Ain Helwan, Cairo, Egypt
E-mail: Nasseramoustafa@yahoo.com

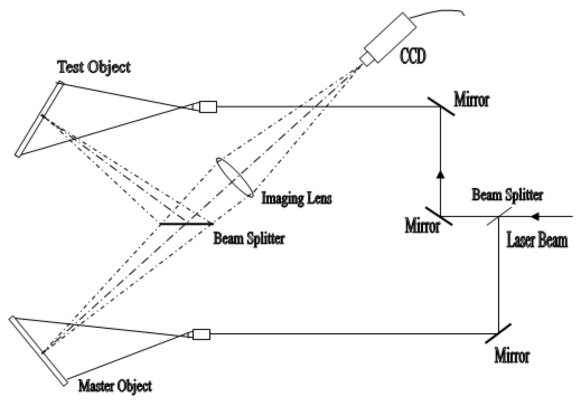

Fig. 1: Schematic diagram of the arrangement.

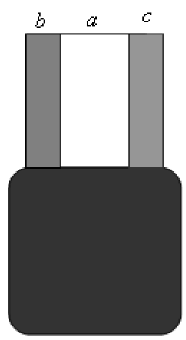

Fig. 2: The master object. (a) movable area. (b) and (c) unmovable area.

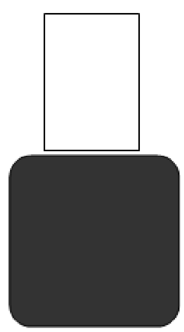

Fig. 3: The test object.

Let U_t is the complex amplitude of the wave field scattered by the test object in its undeformed state.

$$U_{mr} = U_m + U_r \tag{1}$$

$$U_{mr} = a_m \exp j(\phi_m) + a_r \exp j(\phi_r) \tag{2}$$

The intensity distribution of the light at a certain point on the CDD detector array is

$$I = \left| U_t + U_{mr} \right|^2 \tag{3}$$

$$I = |U_t|^2 + |U_{mr}|^2 + U_t U_{mr}^* + U_{mr} U_t^* \tag{4}$$

i.e.

$$I = I_t + I_m + I_r + 2\sqrt{I_t I_m}\cos(\phi_t - \phi_m) + 2\sqrt{I_t I_r}\cos(\phi_t - \phi_r) \tag{5}$$

Where I_t is the intensity distribution of the light scattered by the undeformed state of the test object. I_m and I_r are the intensity distributions of the light scattered by the movable (undeformed), and the fixed areas of the modified master object respectively.

Eq. (5) can be rewritten as follow,

$$I = I_t + I_m + I_r + 2\sqrt{I_t I_m}\cos(\Delta\phi_{tm}) + 2\sqrt{I_t I_r}\cos(\Delta\phi_{tr}) + 2\sqrt{I_m I_r}\cos(\Delta\phi_{mr}) \tag{6}$$

where $\Delta\phi_{tm} = (\phi_t - \phi_m), \Delta\phi_{tr} = (\phi_t - \phi_r)$, and $\Delta\phi_{mr} = (\phi_m - \phi_r)$,

In the second step, we recorded the wave fields scattered by the test and modified master objects respectively in the case of the deformed state.

If the symbols $U_t^{/}$ and $U_m^{/}$ are the complex amplitudes of the wave field scattered by the movable (deformed) areas of the test and modified master object respectively.

$$U_t^{/} = u_t^{/} \exp j(\phi_t + \phi_t^{/}) \tag{7}$$

Also we have

$$U_{mr}^{/} = U_m^{/} + U_r \tag{8}$$

$U_{mr}^{/}$ is the resultant complex amplitude of the wave fields scattered by the movable (deformed) and the fixed area of the master object.

$$U_{mr}^{/} = u_m^{/} \exp j(\phi_m + \phi_m^{/}) + u_r \exp j(\phi_r) \tag{9}$$

where $\phi_t^{/}$ and $\phi_m^{/}$ are the individual phase changes introduced by the movement of the movable areas of the test and master object respectively. The intensity distribution of the light at a certain point on the face plate of the camera is

$$I^{/} = |U_t^{/} + U_{mr}^{/}|^2 \tag{10}$$

$$I^{/} = |U_t^{/}|^2 + |U_{mr}^{/}|^2 + U_t^{/} U_{mr}^{/*} + U_{mr}^{/} U_t^{/*}$$

i.e.

$$I^{/} = I_t^{/} + I_m^{/} + I_r + 2\sqrt{I_t^{/} I_m^{/}}\cos[(\phi_t + \phi_t^{/}) - (\phi_m + \phi_m^{/})] + 2\sqrt{I_t^{/} I_r}\cos[(\phi_t + \phi_t^{/}) - \phi_r] \tag{11}$$

where $I_t^{/}$ and $I_m^{/}$ are the intensity distributions of the light scattered by the movable (deformed) areas of the test and master objects respectively.

Eq. (10) can be simplified as,

$$I^{/} = I_t^{/} + I_m^{/} + I_r + 2\sqrt{I_t^{/} I_m^{/}}\cos(\Delta\phi_{tm} + \Delta\phi_{tm}^{/}) + 2\sqrt{I_t^{/} I_r}\cos(\Delta\phi_{tr} + \phi_t^{/}) \tag{12}$$

The two images are subtracted from each other and the differences ΔI are displayed on the monitor as interference fringe systems. We assume that the deformations of the movable areas of the objects are small enough to maintain that $I_m^{/} \approx I_m$ and $I_t^{/} \approx I_t$.

$$\Delta I = 4\sqrt{I_t I_m}\sin\left(\Delta\phi_{tm} + \tfrac{1}{2}\Delta\phi_{tm}^{/}\right)\sin\left(\tfrac{1}{2}\Delta\phi_{tm}^{/}\right) + 4\sqrt{I_t I_r}\sin\left(\Delta\phi_{tr} + \tfrac{1}{2}\phi_t^{/}\right)\sin\left(\tfrac{1}{2}\phi_t^{/}\right) \tag{13}$$

The first sine term denotes the correlation fringes corresponding to the difference deformation between the movable areas of the test and master object. The second sine term denote the correlation fringes corresponding to the deformation of the movable (deformed) area of the test object. It is of high spatial frequency which sufficiently large to produce unresovable interference fringes which considered in the theoretical treatment as noise terms. The high spatial frequency lead to decrease the visibility of the difference interference pattern which only can be observed.

Comparison of Eq.(11) with the theory[13] shows that the fringes obtained are identical in the form with those obtained using the photographic correlation technique.

3. Condition For The Observation Of Maximum Visibility Fringes:

Difference correlation fringes may be obtained either by the electronic/digital subtraction or addition of the signal corresponding to the image plane intensity distribution of the difference in deformation of the master and test object. It will now be shown that the optimal reference-to-object (master-to-test) intensity ratio changes as a result of the existence of the fixed areas. Our assumption depending on considering that the first term of equation (11) as the fringe signal and the other represent noise. If the mean value and the standard deviation of the speckle pattern corresponding to the fringe signal are given by $<I>$ and σ, then

$$<I> + 2\sigma_{tot} < I_{sat} \tag{14}$$

where I_{sat} is the saturation level of the CCD camera.
The mean value of the speckle pattern is given by,

$$<I> = <I_t> + <I_m> + <I_r> \tag{15}$$

Where

$<I_t>$ is the mean value of the intensity of the scattered light by the movable area of the test object.
$<I_m>$, $<I_r>$ are the mean values of the intensities of the scattered light by the movable and fixed area of the master object respectively.

The total variance of the speckle pattern is given by,

$$\sigma_{tot}^2 = <I^2> - <I>^2 = <I>^2 \quad \sigma_{tot}^2 = \sigma_t^2 + \sigma_m^2 + \sigma_r^2 + 2<I_t><I_m> + 2<I_m><I_r> + 2<I_t><I_r> \tag{16}$$

Here
σ_t^2, is the variance of the intensity of the scattered light by the movable area of the test object.
σ_m^2, σ_r^2 are the variances of the intensities of the scattered light of the movable and fixed area of the master object.

As we can see from Eq. (14), the variances of the intensities of the light scattered by the movable areas of the test and master object are exist with the variance of the intensity of the light scattered by the fixed area of the master object. If $<I_m> = k_{tm}<I_t>$, $<I_r> = k_{rm}<I_m>$, $\gamma_{t,m,r,}=\sigma_{t,m,r}/<I_{t,m,r,}>$, and when two speckled beams are used, we have

$$\gamma_t = \gamma_m = \gamma_r = 1$$

Then Eq. (14) can be written as

$$\sigma_{tot}^2 = <I>^2 [1 + k_{tm}^2 + 2k_{tm} + k_{rm}^2 k_{tm}^2 + 2k_{tm}^2 k_{rm} + 2k_{tm} k_{rm}] \tag{17}$$

By substitution from Eq. (12) into Eq. (10), then

$$<I> + 2[1 + k_{tm}^2 + 2k_{tm} + k_{rm}^2 k_{tm}^2 + 2k_{tm}^2 k_{rm} + 2k_{tm} k_{rm}]^{1/2} = \rho I_{sat} \tag{18}$$

But we have from Eq. (13),

$$<I> = <I_t> [1+k_{tm} + k_{tm} k_{rm}] \tag{19}$$

where k_{tm} is the intensity ratio of the intensities of the scattered light by the movable areas of the master and test object respectively.

k_{rm} is the intensity ratio of the intensities of the scattered light by the fixed and movable area of the master object.

The filtered and rectified signal averaged over many speckles along a line of constant $\Delta\varphi_{tm}^{/}$ will be $<\Delta I^2>$ since the rectifier acts as a square law detector. The resultant signal is then given by

$$S = <\Delta I^2> = 8<I_t><I_m> \sin^2(½\Delta\varphi_{tm}^{/}) \tag{20}$$

The maximum and minimum signal S_{max} and S_{min} are obtained when

$$½\Delta\varphi_{tm}^{/}=(n+½)\pi$$
$$½\Delta\varphi_{tm}^{/} = n\pi$$

respectively, and are given by

$$S_{max}=8<I_t><I_m> \tag{21}$$

$$S_{min} = 0 \tag{22}$$

From Eqs.(17), (18), and (19)

$$S_{\max} = \frac{8k_{tm}\rho^2 I_{sat}^2}{\left[\left(1+k_{tm}+k_{tm}k_{rm}\right)+2\left[\left(1+k_{tm}\right)^2+\left(1+k_{tm}k_{rm}\right)^2+\left(2k_{rm}k_{tm}^2-1\right)\right]^{\frac{1}{2}}\right]^2} \tag{23}$$

Eq.(21) can be given the unnoisy and noisy signals, which resulting from the absence and the existence of the fixed area (noise) respectively. Below, this equation will be verified experimentally.

4. Experimental Verifications:

To check the validity of Eq. (14), we performed the following experimental work using the experimental arrangement in Fig.1. At the beginning we recorded the undeformed and deformed states of the movable area of the master object. After the installation of the test; in the first step the sum of the speckle fields from the undeformed state of the illuminated test object and the scattered speckle fields of the undeformed master object is recorded and stored in the computer memory using CCD camera. In the second step the sum of the speckle fields from the deformed state of the illuminated test object and the scattered speckle fields of the deformed master object is recorded and stored. After the subtraction, correlation fringes can be observed which characterize the difference of the displacement of the master and test object. A differential correlation fringes can be seen on Fig. 4a. which have been obtained with an intensity ratio (I_t/I_m) ≅1. The visibility of the resulting correlation fringes was 0.343. If we record the same correlation fringes in case of existence the fixed area with the movable area of the master object, the resulting correlation fringes can be shown in Figs. 4b and 4c, the visibilities of the correlation fringes of Figs. 4b and 4c are 0.185 and 0.123 respectively. From Figs. 4b and 4c, we can see the decrease in the visibility as result of existence of the unmovable parts. Fig.5 can be shown the relation between the reference-to-object intensity ratio and the visibility of the correlation fringes. As we can see, the reference-to-object intensity ratio is shifted to be 0.8 and 0.6 in case of existence one fixed part and two fixed parts respectively. To measure the quality of the correlograms and phase maps in more detail a modified visibility function (Butters, 1978) was applied:

$$\text{V}=\frac{I_{\max} - I_{\min}}{I_{\text{sat}}},$$

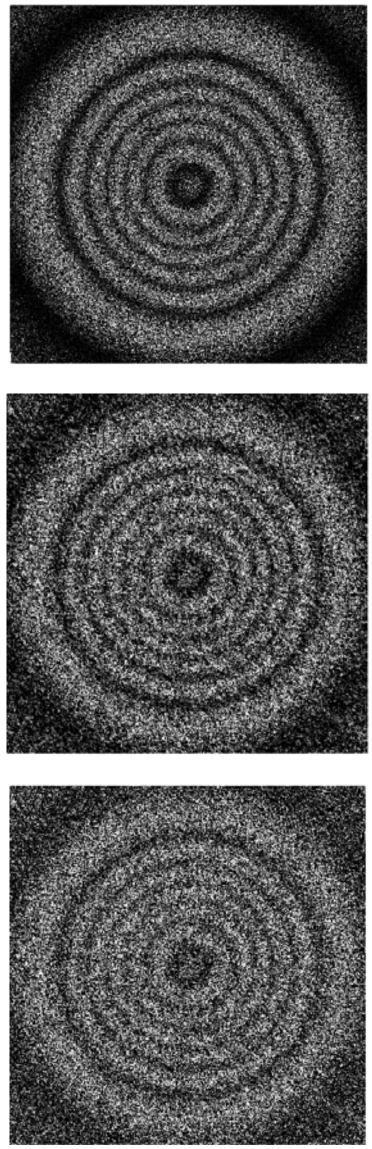

Fig. 4: Photographs of the difference correlation fringes. (a) The movable area. (b) The movable area with one fixed area. (c) The movable area with two fixed areas.

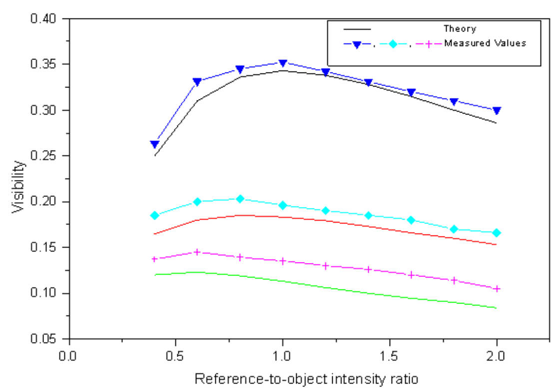

Fig. 5: Visibility of the correlation fringes as a function of the reference-to-object intensity ratio. The upper curves denote the theory, and the lower curves denote the measured values.

where I_{sat} = 255 is the saturation gray level (or saturation intensity) of the imaging system, I_{max} and I_{min} are the maximum and minimum gray levels (or intensities) respectively. The modified visibility function characterizes the electronic speckle pattern interferometry (ESPI) images better than the old function.

5. Conclusion:

The optimum reference-to-object intensity ratio determined for the differential digital speckle pattern interferometry. The optical noise have an effect in changing the optimum reference-to-object intensity ratio. It has also an effect on the degradation of the fringe contrast. The light scattered from the fixed area of the master object can be considered as unwanted reference beams. New formulae have been derived which characterize the effect of the unwanted reference beams (noise) on the displayed differential correlation fringes (fringe signal). There is good agreement achieved between the derived formulae and the experimental results.

REFERENCES

Biedrmann, K., L. Ek and L. Ostland, 1997. Proceedings of the 1974 Strathclyde Conference on the Engineering Uses of Coherent Optics (Cambridge University Press), pp: 219.

Butters, J.N., R. Jones and C. Wykes, 1978. In: Speckle metrology, ed. R.K.Erf (Academic Press).

Creath, K., G.A. Slettemoen, 1985. “Vibration-observation techniques for digital speckle-pattern interferometry,” Jour. of the Opt. Soc. of Am. A, 2(10): 1629.

Ganesan, A.R., C. Joenathan and R.S. Sirohi, 1987. “Real-time comparative digital speckle pattern interferometry,” Opt.Comm., 64(6): 501-506.

János Kornis, Attila Németh, Nasser Moustafa, Ildikó László, 1997. “Application of speckle interferometry for wide scale displacement measurement,” Proc. of Int. Symp. on Automatic Processing of Fringe Patterns, Bremen, pp: 337-339.

Jones, R. and C. Wykes, 1981. “General parameters for the design and optimization of electronic speckle pattern interferometers,” Appl. Opt. 20: A50-1.

Jones, R., C. Wykes (ed.), 1983. “Holographic and speckle interferometry,” Cambridge University Press, Cambridge,” pp: 181.

László, I., J. Kornis, Z. Füzessy, F. Gyímesi, 1997. “Comparative mesurement by speckle interferometry using holographically reconstructed master object,” Opt. Eng. 36(12): 3323-3326.

Lászlo, I., Z. Füzessy, J. Kornis, F. Gyímesi, 1996. “Comparative digital speckle pattern interferometry,” Simulation and Experiment in Laser Metrology (Akademic Verlag, Berlin,1996), pp:146.

Nakadate, S., T. Yatagai, H. Saito, 1980. “Electronic speckle pattern interferometry using digital image processing techniques,” Appl. Opt., 19(11): 1987-1882.

Pederson, H.M., O.J.L.

Slettmoen, G.A., 1979. “General analysis of fringe contrasts in electronic speckle pattern interferometry,” Optica Acta, 26(3): 313-327.

Slettemoen, G.A., 1977. “Optimal processing in electronic speckle pattern interferometry,” Opt.Commu, 23(2): 213-216.